PERGAMON

International Journal of Solids and Structures 38 (2001) 2387–2399

INTERNATIONAL JOURNAL OF SOLIDS and STRUCTURES

www.elsevier.com/locate/ijsolstr

Investigation of minimal forms with conjugate gradient method

B. Maurin [a], R. Motro [b,*]

[a] *Laboratoire d'Etude et de Recherche en Génie Civil, ENSAIS, 24 Bd. de la Victoire, 67000 Strasbourg Cedex, France*

[b] *Laboratoire de Mécanique et Génie Civil, Université Montpellier II, CC 034 - Place Eugene Bataillon, 34095 Montpellier Cedex 5, France*

Received 28 June 1999; in revised form 17 March 2000

Abstract

Amongst the numerous calculation methods available to investigate minimal forms, an approach based on the mechanical consideration of uniform tension in the domain leads to the writing of innovative relationships. Indeed, by establishing the equivalence between the vector of nodal internal forces due to the prestressed domain and the gradient of the function to be minimized, this study proposes to use the conjugate gradient method as a minimal area shape form-finding tool.

The determination of descent directions may refer to Fletcher–Reeves suggestion or to an optimized value based on the Polak–Ribiere formula. Moreover, the steplength calculation is envisaged in accordance with the More and Thuente's line search algorithm or with a modified approach especially adapted to the studied configurations.

Numerical experiments illustrate the use of the conjugate gradient method and thus point out the efficiency of the suggested modifications related to required computation times.

In a second time, the conjugate gradient method is compared with density methods and a mixed formulation is therefore put forward. Numerical tests enable the comparison between these different approaches.

Keywords: Minimal forms; Conjugate gradient

1. Introduction

In view of their intrinsic properties, minimal forms constitute one of the most attractive domains of science. Numerous methods were therefore proposed in order to ensure their form finding.

Based on the geometrical specification of zero mean curvature, we leave aside numerical approaches essentially related to the resolution of Laplace's equation. Major results were found also from physical modeling such as the studies on soap films undertaken by Otto (1973).

* Corresponding author. Tel.: +33-4-6714-3754; fax: +33-4-6714-4555.

E-mail addresses: maurin@corbu01.u-strasbg.fr (B. Maurin), motro@lmgc.univ-montp2.fr (R. Motro).

0020-7683/01/$ - see front matter
PII: S0020-7683(00)00113-X

The other significant property, i.e. uniform tension configuration, has led to several mechanical formulations. We distinguish methods based on non-linear large displacement finite element procedures (Haug, 1987) or on the use of dynamic relaxation (Barnes, 1976; Lewis and Lewis, 1996).

The problem is taken up in this paper with the aim of suggesting new approaches and henceforth innovative shape-finding processes. This paper aims to establish theoretical relationships between internal forces related to the tension of the domain and analytic functions that have to be minimized. Afterwards, the conjugate gradient method is used as an optimization tool which leads to the determination of the searched configurations.

2. Calculation of minimal forms

2.1. Minimal length nets

These configurations are characterized by the mechanical consideration of homogeneous tension in cable elements or by considering that the sum of way length $\mathscr{L}$ is minimal.

The studied structure includes N nodes and C cable elements, c_i elements are adjacent to the node i. Hence, if each element k has a length of ℓ_{ck}, then

$$\mathscr{L} = \sum_{k=1}^{C} \ell_{ck} = \sum_{k=1}^{C} \|\vec{1_k 2_k}\| = \sum_{k=1}^{C} (X_{1_k 2_k}^2 + Y_{1_k 2_k}^2 + Z_{1_k 2_k}^2)^{0.5}, \tag{2.1}$$

where X_{1_k} and X_{2_k} are the global coordinates of the two nodes 1_k and 2_k for the cable element k in the global structure axis $(\vec{X}\,\vec{Y}\,\vec{Z})$ and $X_{2_k 1_k} = X_{2_k} - X_{1_k}$.

We can write $\mathscr{L} = f(\mathscr{X})$, where $\mathscr{X} = \{\mathscr{X}\}$ represents the vector of the nodal coordinates such as $\{\mathscr{X}\}^{\mathrm{T}} = \langle X_1\, Y_1\, Z_1 \ldots X_k\, Y_k\, Z_k \ldots X_N\, Y_N\, Z_N \rangle$. $\mathscr{L}$ has turning values if at each node k we verify

$$\frac{\partial f(\mathscr{X})}{\partial X_k} = \frac{\partial f(\mathscr{X})}{\partial Y_k} = \frac{\partial f(X)}{\partial Z_k} = 0. \tag{2.2}$$

Therefore, it can be written for $\vec{X}$ direction:

$$\frac{\partial f(\mathscr{X})}{\partial X_i} = \frac{\partial \mathscr{L}}{\partial X_i} = \sum_{j=1}^{c_i} \frac{-X_{2_j i}}{\ell_{cj}} = 0 \tag{2.3}$$

with $X_i = X_{1_i}$ (1 being one end of element j, see Fig. 1(a)); similar expressions are valid for $\vec{Y}$ and $\vec{Z}$ directions.

If there exists an homogeneous tension t_0 in the cable net, the residual force $\vec{F}_i$ at node i is

$$\vec{F}_i = \sum_{j=1}^{c_i} t_0\, \vec{x}_j, \tag{2.4}$$

where $\vec{x}_j$ is the norm vector associated to element j. Along the direction $\vec{X}$, we have

$$F_{i_X} = t_0 \sum_{j=1}^{c_i} \frac{X_{2_j i}}{\ell_{cj}}. \tag{2.5}$$

Since equilibrium is reached when components of $\vec{F}_i$ cancel, we find the same expression as for Eq. (2.3) and then it is shown that $\partial\mathscr{L}/\partial X_i = \partial\mathscr{L}/\partial Y_i = \partial\mathscr{L}/\partial Z_i = 0$ is equivalent to $F_{i_X} = F_{i_Y} = F_{i_Z} = 0$.

Therefore, minimization of the cable net length can be replaced by the minimization of the nodal forces $\vec{F}_i$ to zero, which expresses that the uniform tension cable structure is an equilibrated configuration.

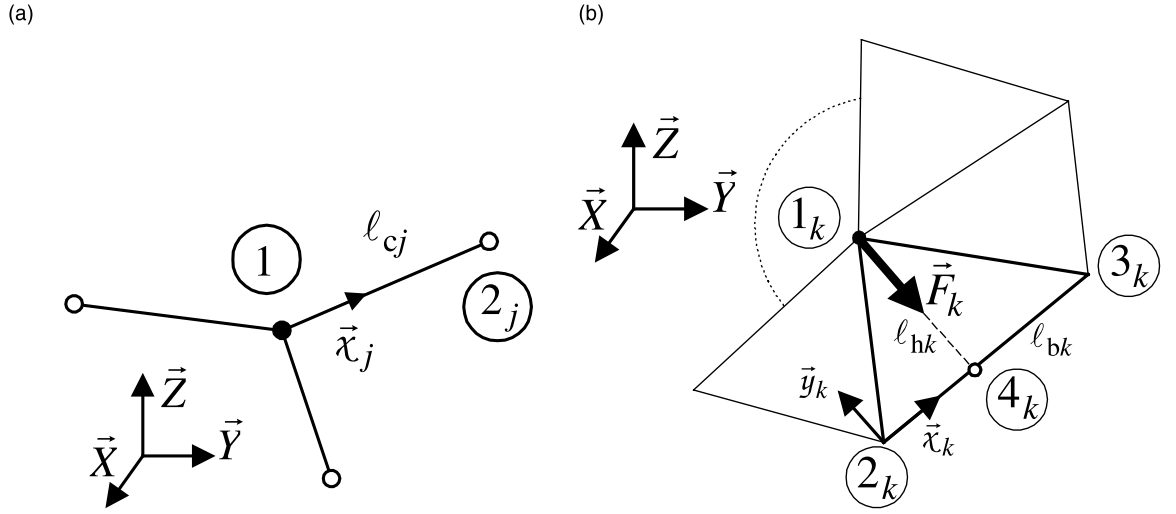

Fig. 1. (a) Cable net and (b) membrane surface element.

We may assume $t_0 = 1$ and consider $\{g(\mathscr{X})\} = -\langle \dots F_{iX} F_{iY} F_{iZ} \dots \rangle^{\mathrm{T}}$ as a vector of nodal internal forces, and the gradient of function $f(\mathscr{X})$ is thus the vector $-g$.

2.2. Minimal surfaces

These minimal area domains rely on the mechanical property of an homogeneous tension in the surface. Configurations are modeled by M membrane surface triangular elements and N nodes; m_i elements are connected to node i.

Hence, the sum of area elements is

$$\mathscr{S} = \sum_{k=1}^{M} s_k \quad \text{with} \quad s_k = \tfrac{1}{2} \ell_{bk} \, \ell_{hk}, \tag{2.6}$$

where by considering the point 4_k such as (Fig. 1(b))

$$\vec{2_k 3_k} \cdot \vec{1_k 4_k} = 0 \quad \text{and} \quad \ell_{bk} = \|\vec{2_k 3_k}\|, \quad \ell_{hk} = \|\vec{1_k 4_k}\|. \tag{2.7}$$

By writing $\mathscr{S} = f(\mathscr{X})$, if each node k coordinates verify $\partial f(\mathscr{X})/\partial X_k = \partial f(\mathscr{X})/\partial X_k = \partial f(\mathscr{X})/\partial Z_k = 0$, then $\mathscr{S}$ is minimal. Hence, with

$$\frac{\partial f(\mathscr{X})}{\partial X_i} = \frac{\partial \mathscr{S}}{\partial X_i} = \frac{1}{2} \sum_{j=1}^{m_i} \left(\frac{\ell_{bj}}{2 \ell_{hj}} \frac{\partial \ell_{hj}^2}{\partial X_i} \right) = -\frac{1}{2} \sum_{j=1}^{m_i} \left(\frac{\ell_{bj}}{\ell_{hj}} X_{4_j i} \right) = 0. \tag{2.8}$$

Under the assumption of an uniform tension surface, internal force at node i may be written as

$$\vec{F}_i = -\sum_{j=1}^{m_i} \frac{\boldsymbol{\sigma}_0 \, \ell_{bj}}{\ell_{hj}} \vec{y}_k, \tag{2.9}$$

where $\boldsymbol{\sigma}_0$ represents the isotropic Cauchy prestress tensor associated to every surface element in its local axis $(\vec{x}_k \, \vec{y}_k \, \vec{z}_k)$ such as

$$\left\{\boldsymbol{\sigma}_{0k_{\mathrm{loc}}}\right\}^{\mathbf{T}} = \left\langle \boldsymbol{\sigma}_{0x_k} | \boldsymbol{\sigma}_{0y_k} | \boldsymbol{\sigma}_{0xy_k} \right\rangle = \langle \boldsymbol{\sigma}_0 | \boldsymbol{\sigma}_0 | 0 \rangle \quad \text{with} \boldsymbol{\sigma}_0 > 0. \tag{2.10}$$

Along the direction $\vec{X}$, it becomes

$$F_{i_X} = \frac{\boldsymbol{\sigma}_0}{2} \sum_{j=1}^{m_i} \frac{\ell_{\mathrm{b}j}}{\ell_{\mathrm{h}j}} X_{4_{ji}}. \tag{2.11}$$

Application of an identical approach along the $\vec{Y}$ and $\vec{Z}$ axes leads to the equivalence between the relationships $\partial \mathscr{S}/\partial X_i = \partial \mathscr{S}/\partial Y_i = \partial \mathscr{S}/\partial Z_i = 0$ and $F_{i_X} = F_{i_Y} = F_{i_Z} = 0$. Likewise in the minimal length nets, calculation of a minimal area may be achieved by searching an equilibrated uniform tension surface.

If $\boldsymbol{\sigma}_0 = 1$, it becomes $\partial f(\mathscr{X})/\partial X_i = -F_{i_X}$, and therefore, the vector of nodal internal forces g is merely opposite to the gradient of function $f(\mathscr{X})$.

Therefore, the problem is to minimize the function of $3N$ variables $\min f(\mathscr{X})$, where $f(\mathscr{X}) = \mathscr{L}$ or $f(\mathscr{X}) = \mathscr{S}$. Since the gradient of $f(\mathscr{X})$ is equal to the internal force vector $-g$, we encounter here a problem of optimization which may be solved by using the *conjugate gradient method*.

3. Conjugate gradient method

3.1. General considerations

Conjugate gradient method can be applied to minimize a non-linear function f by considering its gradient g within an iterative process in the form of

$$\mathscr{X}_{p+1} = \mathscr{X}_p + \alpha_p d_p \quad \text{with } d_p = \begin{cases} -g_p & \text{for } p = 1, \\ -g_p + \beta_p d_{p-1} & \text{for } p \geqslant 2, \end{cases} \tag{3.1}$$

where β_p is a scalar and α_p is a steplength obtained by means of a one-dimensional search for descent direction and called exact line search.

Vector d_p is a descent direction if $\langle g_p, d_p \rangle < 0$, where $\langle . \ , \ . \rangle$ is the scalar product. This relationship may be written as:

$$f'_p(0) < 0 \tag{3.2}$$

with $f'_p(\alpha_p) = \langle g_p(\alpha_p), d_p \rangle$, since we consider functions of the scalar α_p verifying

$$f_p(\alpha_p) = f_p(\mathscr{X}_p + \alpha_p d_p) \quad \text{and} \quad g_p(\alpha_p) = g_p(\mathscr{X}_p + \alpha_p d_p). \tag{3.3}$$

We note that $f_p(0) = f_p$ and $g_p(0) = g_p$.

Moreover, the requirement $f_{p+1} < f_p$ translating decrease of f at each iteration is unsatisfactory since the decrease can be negligible when compared with reduction which can be obtained in an optimum reduction process based on exact line search. This exact line search supposes that α_p satisfies the Strong Wolfe conditions:

$$f_p(\alpha_p) \leqslant f_p(0) + \mu \alpha_p f'_p(0) \quad \text{and} \quad |f'_p(\alpha_p)| \leqslant \eta |f'_p(0)| \quad \text{with } 0 < \mu < \eta < \tfrac{1}{2}. \tag{3.4}$$

Values for β_p were proposed by Fletcher–Reeves (1972) and Polak–Ribiere (1969):

$$\beta_p^{\mathrm{FR}} = \frac{\langle g_p, g_p \rangle}{\langle g_{p-1}, g_{p-1} \rangle} \geqslant 0 \quad \text{and} \quad \beta_p^{\mathrm{PR}} = \frac{\langle g_p, g_p - g_{p-1} \rangle}{\langle g_{p-1}, g_{p-1} \rangle}. \tag{3.5}$$

"FR" and "PR" are used in the following text for Fletcher–Reeves and Polak–Ribiere methods. Since numerical performance of FR method is often slower than the PR method, Al Baali (1985) demonstrated

that, if the FR process satisfies the Strong Wolfe conditions (3.4), it becomes $\langle g_p, d_p\rangle \leqslant -\tau\langle g_p, g_p\rangle$ with τ positive value, and therefore, the requirement $f'_p(0) < 0$ is satisfied. Moreover, Zoutendijk (1970) pointed out the global convergence on general functions for the FR method and also proved that it cannot fail.

Gilbert and Nocedal (1992) took an interest in the PR method. Their study enhanced two main considerations. Firstly, the specification $|\beta_p^{\mathrm{PR}}| \leqslant \beta_p^{\mathrm{FR}}$ leads to the global convergence of the method. Such a process is called "PR method constrained by the FR method".

Secondly, a comment based on a suggestion by Powell (1986), allows the use of only non-negative β_p^{PR} values. It is related to the sufficient descent condition $\langle g_p, d_p\rangle \leqslant -\omega\langle g_p, g_p\rangle$ with $0 < \omega \leqslant 1$ and equation

$$\langle g_p, d_p\rangle \leqslant -\langle g_p, g_p\rangle + \beta_p^{\mathrm{PR}}\langle g_p, d_{p-1}\rangle. \tag{3.6}$$

The specification $\langle g_p, g_{p-1}\rangle \leqslant \langle g_p, g_p\rangle$ from Eq. (3.5), while SW conditions (3.4) are satisfied, provides $\liminf \langle g_p, g_p\rangle = 0$ and therefore the global convergence of the method.

Our numerical experiments aim to compare these two approaches: the FR method and an optimized PR method (see Section 3.2.4) where Gilbert and Nocedal's considerations are given due consideration:

$$\beta_p^{\mathrm{OP}} = \min\left\{\beta_p^{\mathrm{FR}}, \beta_p^{\mathrm{PR}^+}\right\} \quad \text{with } \beta_p^{\mathrm{PR}^+} = \max\left\{\beta_p^{\mathrm{PR}}, 0\right\}. \tag{3.7}$$

3.2. Line search procedures

3.2.1. Principle

The main problem is to find an acceptable steplength α_p which obeys the SW conditions. Numerous procedures have been proposed and they are mainly related to line search algorithms which generate a sequence of estimate α_{p_k} and end when a convenient point satisfies the required conditions.

Gilbert and Nocedal emphasize on the efficiency of the approach suggested by More and Thuente (1990). This method aims to find an acceptable α_{p_k} in the sense that it belongs to the set $T_p(\mu)$ defined by

$$T_p(\mu) = \left\{\alpha_p > 0 : f_p(\alpha_p) \leqslant f_p(0) + \mu\alpha_p f'_p(0) \quad \text{and} \quad \left|f'_p(\alpha_p)\right| \leqslant \mu\left|f'_p(0)\right|\right\}. \tag{3.8}$$

Given α_{p_0} in $\left[\alpha_{p_{\min}}, \alpha_{p_{\max}}\right]$, the search algorithm generates a sequence of nested intervals $\left\{I_{p_k}\right\}$ and a sequence of iterative values α_{p_k} in this interval until it belongs to $T_p(\mu)$.

The lower bound $\alpha_{p_{\min}}$ is specified by the user and the upper bound $\alpha_{p_{\max}}$ may be evaluated according to

$$\alpha_{p_{\max}} = \frac{1}{\mu}\frac{f_p(0) - f_{p_{\min}}}{-f'_p(0)} \tag{3.9}$$

and thus corresponds to the point at which the μ-line of equation $f_p(0) = -\mu\alpha_p f'_p(0)$ intersects the line $f_p(\alpha_p) = f_{p_{\min}}$, where $f_{p_{\min}}$ is the lower value on $f_p(\alpha_p)$ also supplied by the user.

A last remark is that the updating process needs the definition of the auxiliary function:

$$\mathbf{\Psi}_p(\alpha_p) = f_p(\alpha_p) - f_p(0) - \mu\alpha_p f'_p(0) \tag{3.10}$$

and its derivative $\mathbf{\Psi}'_p(\alpha_p)$.

3.2.2. Algorithm

With $\alpha_{p_{\min}} = 0$ and thus $\left\{I_{p_0}\right\} = \left[\alpha_{pi_0}, \alpha_{ps_0}\right] = \left[0, \alpha_{p_{\max}}\right]$ the algorithm is for $k = 1, 2, \ldots$

(i) Choose a trial value $\alpha_{pt_k} \in \left[\alpha_{pi_{k-1}}, \alpha_{ps_{k-1}}\right]$. If α_{pt_k} verifies the SW conditions (3.4), then $\alpha_p^{\mathrm{MT}} = \alpha_{pt_k}$ (end of process).

(ii) *Case MT*$_1$: if $\mathbf{\Psi}_p(\alpha_{pt_k}) > \mathbf{\Psi}_p(\alpha_{pi_{k-1}})$, then $\alpha_{pi_k} = \alpha_{pi_{k-1}}$ and $\alpha_{ps_k} = \alpha_{pt_k}$. (3.11)

$$\textit{Case } MT_2\text{: if } \boldsymbol{\Psi}_p(\alpha_{pt_k}) \leqslant \boldsymbol{\Psi}_p(\alpha_{pi_{k-1}}) \text{ and } \boldsymbol{\Psi}'_p(\alpha_{pt_k})\,(\alpha_{pi_{k-1}} - \alpha_{pt_k}) > 0, \text{ then } \alpha_{pi_k} = \alpha_{pt_k} \text{ and } \alpha_{ps_k} = \alpha_{ps_{k-1}}. \tag{3.12}$$

$$\textit{Case } MT_3\text{: if } \boldsymbol{\Psi}_p(\alpha_{pt_k}) \leqslant \boldsymbol{\Psi}_p(\alpha_{pi_{k-1}}) \text{ and } \Psi'_p(\alpha_{pt_k})\,(\alpha_{pi_{k-1}} - \alpha_{pt_k}) < 0, \text{ then } \alpha_{pi_k} = \alpha_{pt_k} \text{ and } \alpha_{ps_k} = \alpha_{pi_{k-1}}. \tag{3.13}$$

3.2.3. Comments

Comment 1: As long as case MT_2 holds, the sequence $\alpha_{pt_1}, \alpha_{pt_2} \ldots$ increases while trial values are generated in $\left[\alpha_{pi_{k-1}}, \alpha_{p_{\max}}\right]$ and eventually requires the use of $\alpha_{p_{\max}}$ as a trial value; this is achieved with

$$\alpha_{pt_k} = \min\left\{\alpha_{pi_{k-1}} + \delta_{\max}(\alpha_{pt_{k-1}} - \alpha_{pi_{k-1}}),\, \alpha_{p_{\max}}\right\}, \quad \text{where } \delta_{\max} \in [1.1\,,\, 4]. \tag{3.14}$$

The algorithm ends at $\alpha_{p_{\max}}$ if $\boldsymbol{\Psi}_p(\alpha_{p_{\max}}) \leqslant 0$ and $\boldsymbol{\Psi}'_p(\alpha_{p_{\max}}) < 0$.

Comment 2: If case MT_1 occurs, the sequence of trial values decreases and we force the procedure to use $\alpha_{p_{\min}}$ as a trial value by choosing

$$\alpha_{pt_k} \in \left[\alpha_{p_{\min}}, \max\left\{\delta_{\min}\,\alpha_{pi_{k-1}}, \alpha_{p_{\min}}\right\}\right] \quad \text{with } \delta_{\min} < 1 \tag{3.15}$$

(More and Thuente recommend $\delta_{\min} = 7/12$). The algorithm stops at $\alpha_{p_{\min}}$ if $\boldsymbol{\Psi}'_p(\alpha_{p_{\min}}) > 0$ or $\boldsymbol{\Psi}_p(\alpha_{p_{\min}}) \geqslant 0$.

Comment 3: The choice $\alpha_{pt_k} \in \left[\alpha_{pi_{k-1}}, \alpha_{ps_{k-1}}\right]$ can be made in any way, but an optimized value is reached when it minimizes, in the given interval, a cubic polynomial interpolating $f_p(\alpha_{pt_k})$, $f'_p(\alpha_{pt_k})$, $f_p(\alpha_{pt_{k-1}})$ and $f'_p(\alpha_{pt_{k-1}})$. In order to simplify calculations, we will take in our numerical experiments the point located at the middle of the interval.

Comment 4: Since we are not able to supply the value of $f_{p_{\min}}$, the choice done by $f_{p_{\min}} = 0.8\, f_p(0)$ appears as a reasonable setting regarding the test examples undertaken.

3.2.4. Application to tension structures

Application of the More and Thuente's line search algorithm to the specific case of tension structures leads to effective and reliable results. Nevertheless, our aim is to suggest a modified approach especially adapted to the computation of minimal forms in order to lower the computation times required by search of the acceptable steplength value. The first proposal refers to the evaluation of $\alpha_{p_{\max}}$.

Since value of $f'_p(0)$ decreases while p increases, $\alpha_{p_{\max}}$ may reach high values. In order to decrease this value, the suggestion is to choose

$$\alpha^{\mathrm{OP}}_{p_{\max}} = \frac{f_p(0) - f_{p_{\min}}}{-f'_p(0)} \tag{3.16}$$

which corresponds to the intersecting point between the μ-line (with $\mu = 1$) and the line $f_p(\alpha_p) = f_{p_{\min}}$. If we verify $f'_p(\alpha^{\mathrm{OP}}_{p_{\max}}) > 0$, the value is accepted; in other cases, $\alpha_{p_{\max}}$ defined by More and Thuente in Eq. (3.9) is chosen.

The second idea deals with the iterative bracketing phase of intervals $\left\{I_{p_k}\right\}$. Instead of cases MT_1 to MT_3, we propose to consider

$$\textit{Case } MT_1^{OP}\text{: if } f'_p(\alpha_{pt_k}) \geqslant 0, \text{ then } \alpha_{pi_k} = \alpha_{pi_{k-1}} \text{ and } \alpha_{ps_k} = \alpha_{pt_k}. \tag{3.17}$$

$$\textit{Case } MT_2^{OP}\text{: if } f'_p(\alpha_{pt_k}) < 0 \text{ then } \alpha_{pi_k} = \alpha_{pt_k} \text{ and } \alpha_{ps_k} = \alpha_{ps_{k-1}}. \tag{3.18}$$

The comments 1–4 written for the More–Thuente's algorithm are still in use. The final acceptable value is denoted α^{OP}_p.

3.3. Numerical experiments

Several illustrative examples are presented in order to compare the different approaches. Calculation of the scalar β_p may be envisaged with the Fletcher–Reeves formula (β_p^{FR} from Eq. (3.5)) or by using the optimized suggested value (β_p^{OP} as in Eq. (3.7)).

Moreover, the steplength evaluation may refer to the More–Thuente's line search algorithm (α_p^{MT}) or with respect to the modified method previously put forward (α_p^{OP}) in Section 3.2.

All the tests are performed with $\mu = 10^{-3}$ and $\eta = 10^{-1}$ in the Strong Wolfe conditions (3.4). Gilbert and Nocedal have indeed demonstrated that this choice for η ensures that the methods FR and PR constrained by the FR are globally convergent since with a steplength satisfying the SW conditions, it verifies

$$\frac{-1}{1-\eta} \leqslant \frac{\langle g_p, d_p\rangle}{\langle g_p, g_p\rangle} \leqslant \frac{2\eta - 1}{1-\eta}.$$

The choice for μ was presented as a reasonable value by More and Thuente; actually, the general trend is that the necessary number of evaluation for α is decreasing, if μ decreases. This explains our choice for μ. Furthermore, the searched minimal form is considered as reached if at each node i of the configuration we verify $(\langle F_i, F_i\rangle)^{0.5} \leqslant 10^{-3}$.

3.3.1. Minimal length net calculations

First application illustrates a simple example where a minimal net is performed between four fixed nodes located on the vertices of a $d \times d$ square. Two free nodes connected to five cable elements lie in the square. Initial configuration is represented in Fig. 2(a) and the resulting minimal geometry in Fig. 2(b).

CPU computation times are presented in Table 1 in the form of β_p calculation method/α_p algorithm (OP/MT refers to β_p^{OP} and α_p^{MT}). Numbers are normalized in such a way that OP/OP corresponds to 1 since it appears as the fastest procedure.

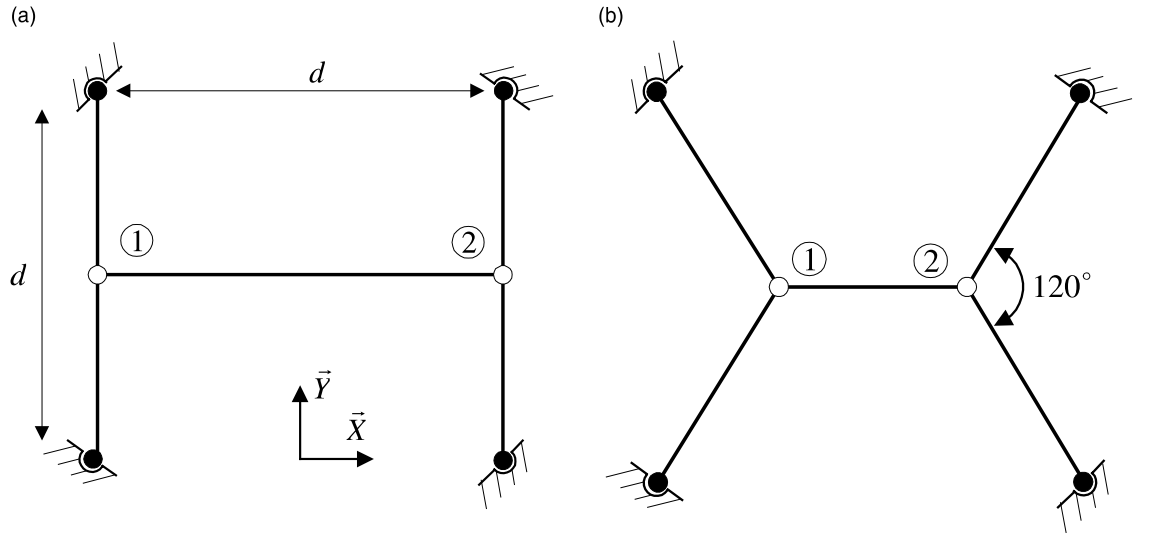

Fig. 2. (a) Square initial configuration and (b) square minimal geometry.

Table 1
Comparison between conjugate gradient procedures

Calculation procedure		Square	Schwarz's saddle	Pseudo-HP	Scherk's surface	Chinese hat	Performances
β_p	α_p						
FR	MT	2.3	5.3	3.0	4.6	4.4	3.92
OP	MT	1.9	3.8	2.2	3.6	2.5	2.8
FR	OP	1.2	1.4	1.3	1.5	1.4	1.35
OP	OP	1.0	1.0	1.0	1.0	1.0	1.00

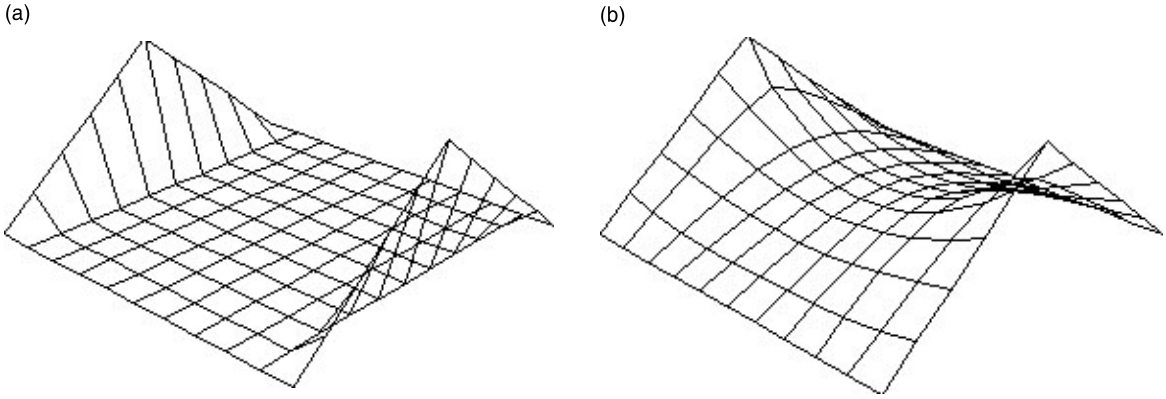

Fig. 3. (a) Schwarz's saddle: initial mesh and (b) Schwarz's saddle.

The second example describes investigation of Schwarz's saddle shape. Fig. 3 shows the initial and final configurations.

3.3.2. Minimal surface investigations

The first test is devoted to the calculation of a well-known minimal configuration improperly called hyperbolic paraboloid since this appellation is indeed geometrically related to a ruled surface which cannot satisfy the condition of zero mean curvature and therefore is no more a minimal area surface. Hence, we propose to denominate this domain as a pseudo-hyperbolic paraboloid (Fig. 4). Another minimal form is represented in Fig. 5; this domain is inspired by the Scherk's surface.

The next example illustrates the shape-finding of a form called "Chinese hat". A soap film takes place between two parallel rings of radii 10 and 2 m and distant from the height $h = 4$ m (Fig. 6(a) and (b)).

The last test aims to point out a possible divergence of the procedure when boundary conditions do not allow to generate a minimal surface. It is derived from the Chinese hat example, when the distance separating the rings is too important. This non-convergent test is represented in Fig. 6(c) where $h = 6$ m.

3.3.3. Comparison between conjugate gradient approaches

Computation times, presented in Table 1, are summarized under the heading "Performances" and the analysis leads to the following comments. Methods based on the use of β_p^{FR} appear clearly as less efficient than procedures with β_p^{OP} (with a factor close to 1.4). This trend confirms the results given by Gilbert and Nocedal on a collection of large test problems.

Moreover, the use of the optimized line search procedure allows to reduce CPU times to about 2.8 when compared with the use of More–Thuente's algorithm. This reduction is related to the specification of a

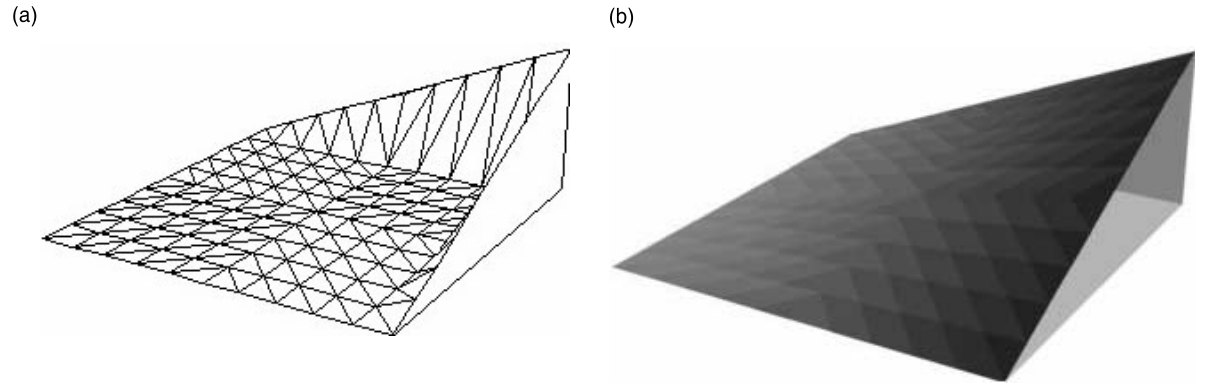

Fig. 4. (a) Pseudo-HP initial configuration and (b) pseudo-HP surface.

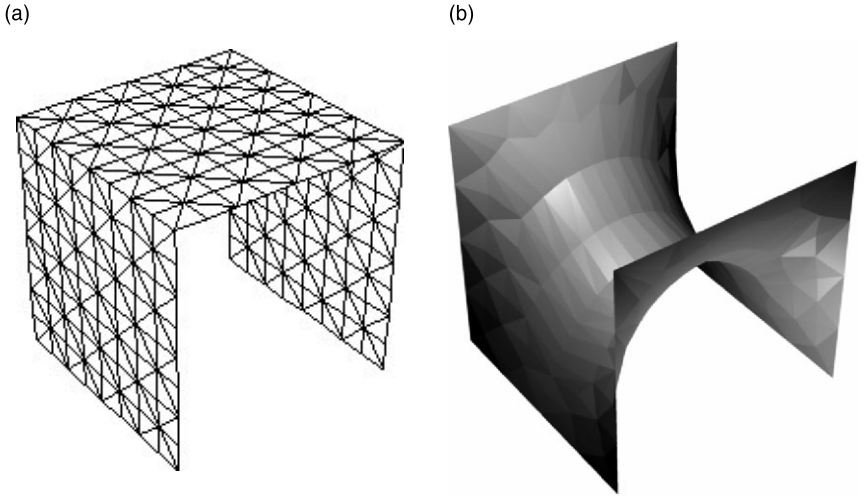

Fig. 5. (a) Pseudo-Scherk's surface initial mesh and (b) pseudo-Scherk's minimal surface.

narrower initial interval (with $\alpha_{p_{\max}}^{\mathrm{OP}}$ instead of $\alpha_{p_{\max}}$) and also to non-calculation of functions $\mathbf{\Psi}_p(\alpha_p)$ and $\mathbf{\Psi}'_p(\alpha_p)$ within the bracketing phase.

Since we do not desire to draw any firm conclusions from these results, the interesting feature is that the suggested optimized approaches provide faster methods devoted to minimal form calculations.

4. Conjugate gradient and density methods

4.1. Calculation of minimal forms with density methods

These approaches originate from the mechanical consideration of a homogeneous tension distribution in the net or in the surface.

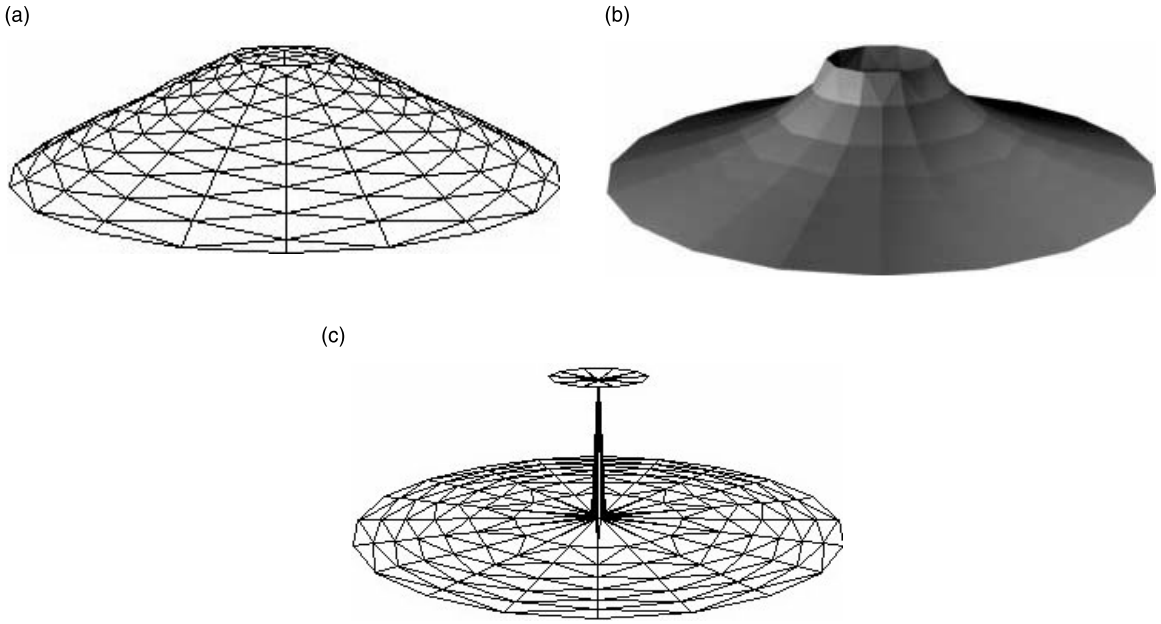

Fig. 6. (a) Chinese hat: initial configuration, (b) Chinese hat and (c) divergent computation.

Minimal length net investigation is related to the process suggested by Linkwitz and Sheck (1971) and called *force density method*. The ratio between the tension and the length of each cable element is prescribed by the designer in the form of

$$q_{\ell k} = \frac{t_{0k}}{\ell_{ck}}. \tag{4.1}$$

Thus, an iterative procedure devoted to the calculation of a t_0 uniform tension net and consequently a minimal length net was put forward:

DE_ℓ^1: initialize force density coefficients with $q_{\ell k}^{(p=1)} = 1$. (4.2)

DE_ℓ^2: calculate equilibrated configuration and evaluate the resulting cable tensions by

$$t_{0k}^{(p)} = q_{\ell k}^{(p)}\, \ell_{ck}^{(p)}. \tag{4.3}$$

DE_ℓ^3: if for all elements $\left|t_0 - t_{0k}^{(p)}\right| < \textit{tolerance}$, then the minimal form is obtained.

$$\text{Else, modify FD coefficients with } q_{\ell k}^{(p+1)} = q_{\ell k}^{(p)}\, \frac{t_0}{t_{0k}^{(p)}} \text{ and return to } \mathrm{DE}_\ell^2. \tag{4.4}$$

The attention may be focused on the first step DE_ℓ^1 where identical force density coefficients are specified. Sheck demonstrated that such a requirement leads to the calculation of a specific geometry whose main property is to minimize the sum of squares of the cable lengths. Steps DE_ℓ^2 and DE_ℓ^3 deal with an iterative strategy where convenient adapted FD coefficients are taken in order to obtain the searched uniform tension net.

Concerning minimal surface calculation, the chosen technique is the *surface stress density method* which appears as an extension of the force density method to the bidimensional case of prestress membrane

surfaces (Maurin and Motro, 1998). The domain is composed of triangular elements characterized by an isotropic Cauchy stress tensor such as, for every k element

$$\left\{\boldsymbol{\sigma}_{0k_{\mathrm{loc}}}\right\}^{\mathrm{T}} = \left\langle \boldsymbol{\sigma}_{0x_k} | \boldsymbol{\sigma}_{0y_k} | \boldsymbol{\sigma}_{0xy_k} \right\rangle = \langle \boldsymbol{\sigma}_{0k} | \boldsymbol{\sigma}_{0k} | 0 \rangle \quad \text{with } \boldsymbol{\sigma}_{0k} > 0. \tag{4.5}$$

Form finding is achieved by prescribing the ratio denoted as surface stress density coefficient (where s_k represents the area of the element k):

$$q_{sk} = \frac{\boldsymbol{\sigma}_{0k}}{s_k}. \tag{4.6}$$

An iterative process was proposed in order to calculate a $\boldsymbol{\sigma}_0$ uniform stress distribution and therefore a minimal surface.

DE_s^1: set surface stress density coefficients to $q_{sk}^{(p=1)} = 1$. (4.7)

DE_s^2: compute the equilibrated structure and thus the prestress distribution with

$$\boldsymbol{\sigma}_{0k}^{(p)} = q_{sk}^{(p)} s_k^{(p)}. \tag{4.8}$$

DE_s^3: if for all elements $\left|\boldsymbol{\sigma}_0 - \boldsymbol{\sigma}_{0k}^{(p)}\right| < \textit{tolerance}$, end of process.
Else, return to DE_s^2 with

$$q_{sk}^{(p+1)} = q_{sk}^{(p)} \boldsymbol{\sigma}_0 / \boldsymbol{\sigma}_{0k}^{(p)}. \tag{4.9}$$

We can demonstrate that the specification of identical surface stress density coefficients which occurs in stage DE_s^1 generates a geometry that minimizes the sum of squared area of the elements.

4.2. Combined approach

The purpose is to provide the designer with a combined approach between conjugate gradient and density methods. For minimal length nets, it consists in replacing the iterative density procedures DE_ℓ^2 to DE_ℓ^3 by the minimization of the function $f(\mathscr{X}) = \mathscr{L}$ with the use of conjugate gradient method described in Section 3.

An identical approach may be envisaged for minimal area surfaces where iterative steps DE_s^2 and DE_s^3 are replaced by minimization according to conjugate gradient with $f(\mathscr{X}) = \mathscr{S}$.

4.3. Numerical results

4.3.1. Scope of the study

We keep the tests described in Section 3.3. Here, the minimal forms are calculated according to the three suggested procedures:

- comprehensive density methods (DE_ℓ^1 to DE_ℓ^3 or DE_s^1 to DE_s^3),
- conjugate gradient method with β_p^{OP} and α_p^{OP} (which appears as the fastest process as shown in Section 3.3.2),
- The combined approaches (DE_ℓ^1 or DE_s^1 followed by the conjugate gradient method with $f(\mathscr{X}) = \mathscr{L}$ or $\mathscr{S}$ and β_p^{OP}, α_p^{OP}).

4.3.2. Results

Computation times are presented in Table 2; they are normalized so that the mixed formulation DE/CG corresponds to 1. The first comment deals with the case of "square" and "pseudo-HP" structures. Density methods and combining approaches provide identical performances; this result may be interpreted by

Table 2
Comparison between conjugate gradient and density methods

	CG	DE	DE/CG
Square	1.2	1.0	1.0
Schwarz's saddle	1.8	0.8	1.0
Pseudo-HP	1.4	1.0	1.0
Scherk's surface	2.7	0.9	1.0
Chinese hat	2.6	1.1	1.0
Performances	1.94	0.96	1.00

considering that forms calculated at stages DE_ℓ^1 or DE_s^1 are geometrically very close to the searched minimal shape.

Concerning the other tests, performances of density and mixed methods appear to be comparable with a slight advantage for the density methods. An explanation may be suggested and concerns the loss of time related to the storage of vectors g_{p-1}, g_p, d_{p-1} and d_p while density procedures only require storage of vector $q_{\ell,s}^{(p-1)}$.

This comment may also explain only partially the lower performances of the conjugate gradient method. Numerical results actually enhanced the need of further investigations according to several concepts such as the influence of the initial mesh or the possibility to use restart procedures in conjugate gradient method (as suggested by Powell, 1977).

5. Conclusion

New processes devoted to the shape-finding of minimal forms are put forward in this paper. The use of conjugate gradient method as an optimization tool devoted to the determination of uniform tension domains leads to effective results. However, the suggestion of modified formulations regarding the descent direction vectors and the steplengths enables to improve the calculation times.

Then, a combined approach including conjugate gradient method and density methods is proposed. Numerical experiments illustrate the close performances existing between this mixed formulation and density methods. We also point out the need of further developments in order to improve the conjugate gradient method efficiency.

Moreover, several future prospects may be enhanced: comparison of the proposed method with other strategies such as dynamic relaxation, particularly by focusing on the relationship between computation times and parameters like convergence tolerance level and also numbers of degree of freedom.

References

Al Baali, M., 1985. Descent property and global convergence of the Fletcher–Reeves method with inexact line search. IMA J. Numer. Anal. 5, 121–124.

Barnes, M.R., 1976. Form-finding of minimum surface membranes. International Association for Shell and Spatial Structures World Congress on Space Enclosures, University of Montreal, pp. 115–124.

Fletcher, R., Reeves, C.M., 1972. Function minimization by conjugate gradient method. IBM J. Res. Develop. 16, 431–433.

Gilbert, J.C., Nocedal, J., 1992. Global convergence properties of conjugate gradient methods for optimization. SIAM J. Optim. 2 (1), 21–42.

Haug, E., 1987. Numerical calculation of minimal surfaces, IL 18, 370–380.

Lewis, W.J., Lewis, T.S., 1996. Application of formian and dynamic relaxation to the form-finding of minimal surfaces. J. IASS 37, 165–186.

Linkwitz, K., Sheck, H.J., 1971. Einige bemerkungen von vorgespannten seilnetzkonstruktionen. Ingenieur Archiv 40, 145–158.
Maurin, B., Motro, R., 1998. Investigation of minimal forms with density methods. J. IASS 38, 143–154.
More, J.J., Thuente D.J., 1990. On line search algorithms with guaranted sufficient decrease. Math. Comp. Sci. Div., Argonne National Laboratory, Argonne, IL. Preprint MCS-P153-0590.
Otto, F. (Ed.), 1973. Tensile Structures, vols. 1 and 2, MIT, Cambridge, MA.
Powell, M.J.D., 1977. Restart procedures for the conjugate gradient method. Math. Program. 12, 241–254.
Powell, M.J.D., 1986. Convergence properties of algorithms for nonlinear optimization. SIAM Rev. 28, 487–500.
Zoutendijk, G., 1970. Nonlinear programming computational methods. In: Abadie, J. (Ed.), Integer and Nonlinear Programming. North Holland, Amsterdam. pp. 37–86.